Supplemental Information for

Unraveling a black box: An open-source methodology for the field calibration of small air quality sensors

Seán Schmitz[1], Sherry Towers[1], Guillermo Villena[2], Alexandre Caseiro[1], Robert Wegener[3], Dieter Klemp[3], Ines Langer[4], Fred Meier[5], and Erika von Schneidemesser[1]

[1] Institute for Advanced Sustainability Studies e. V. (IASS), Berliner Strasse 130, 14467 Potsdam, Germany
[2] Bergische Universität Wuppertal, Physikalische und Theoretische Chemie/FK4, Gaussstrasse 20, 42119 Wuppertal, Germany
[3] Forschungszentrum Jülich GmbH, Institute of Energy and Climate Research, IEK8: Troposphere, 52425 Jülich, Germany, Germany
[4] Freie Universität Berlin, Institut für Meteorologie, Carl-Heinrich-Becker Weg 6-10, 12165 Berlin, Germany
[5] Chair of Climatology, Institute of Ecology, Technische Universität Berlin, Rothenburgstraße 12, D-12165 Berlin, Germany

Contents:

1. Comparison of reference instruments with Forschungszentrum Jülich

2. Map of the measurement site

3. Final results from using s72 in the Winter Campaign, 2018

S1. Comparison of ref instruments with FZ Jülich
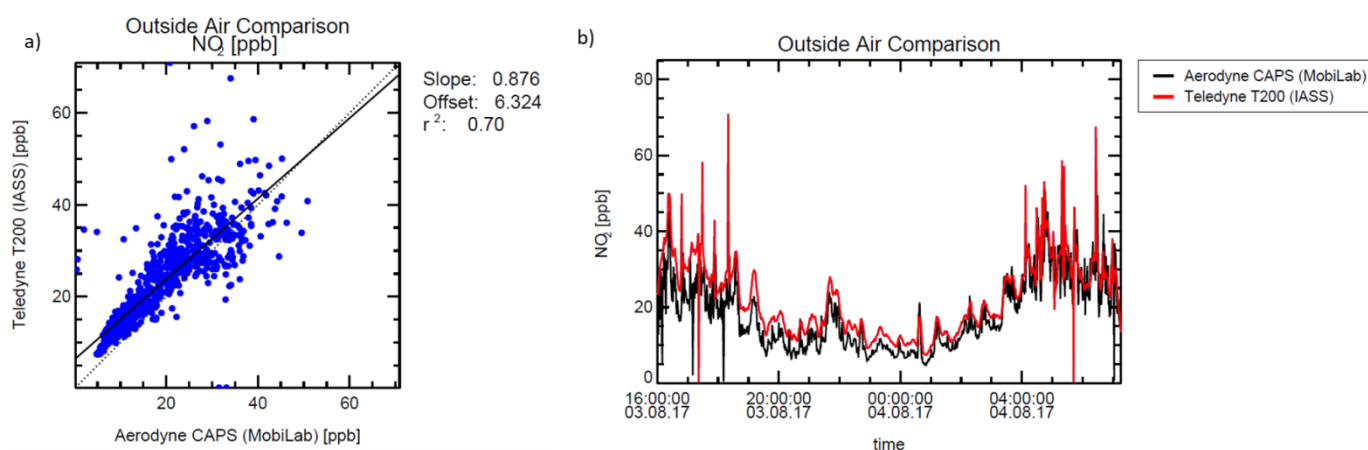
Figure S1. Intercomparison of the T-200 NO$_2$ concentrations with the CAPS (Aerodyne, U.S.A.) from Forschungszentrum Jülich. The data are presented as: a) a scatter plot to establish a correction factor, and b) a time series plot showing the comparison between the two instruments and the range selected for the correction factor.
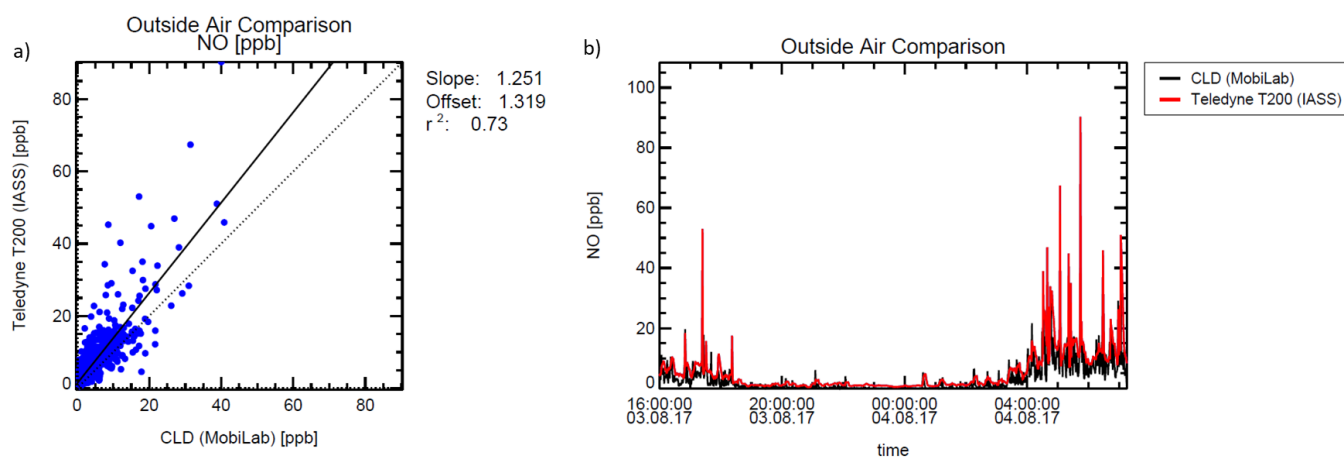
Figure S2. Intercomparison of the T-200 NO concentrations with the CLD 770 AL ppt (ECO Physics, Switzerland) from Forschungszentrum Jülich. The data are presented as: a) a scatter plot with selected data to establish a correction factor, and b) a time series plot showing the comparison between the two instruments and the range selected for the correction factor.
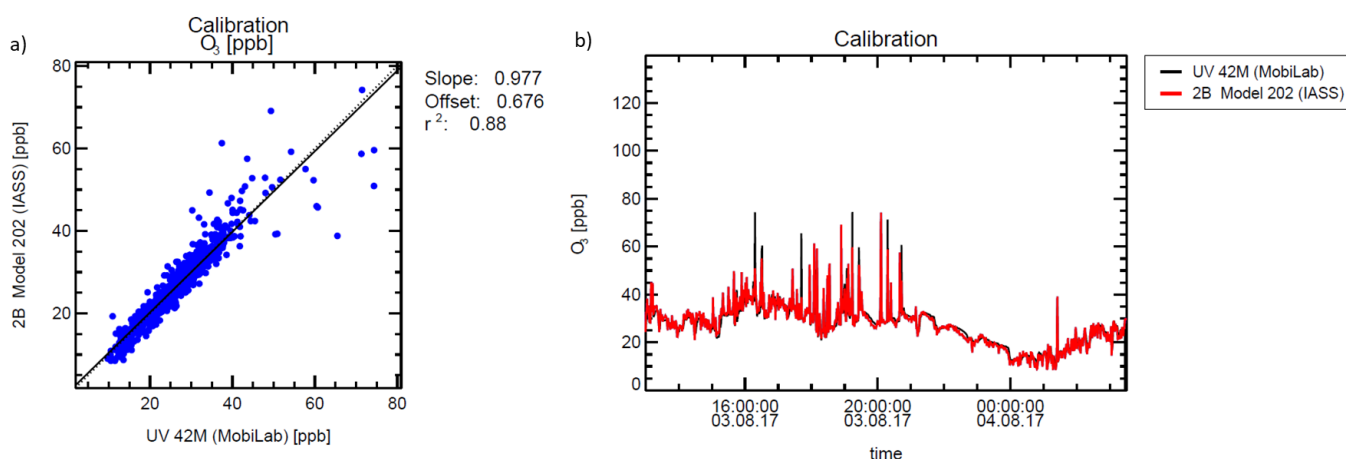
Figure S3. Intercomparison of the Tech 2B Ozone Monitor O₃ concentrations with the O242M (Environnement S.A., France) from Forschungszentrum Jülich. The data are presented as: a) a scatter plot of all data to establish a correction factor, and b) a time series plot showing the comparison between the two instruments.

S2. Map of the measurement site
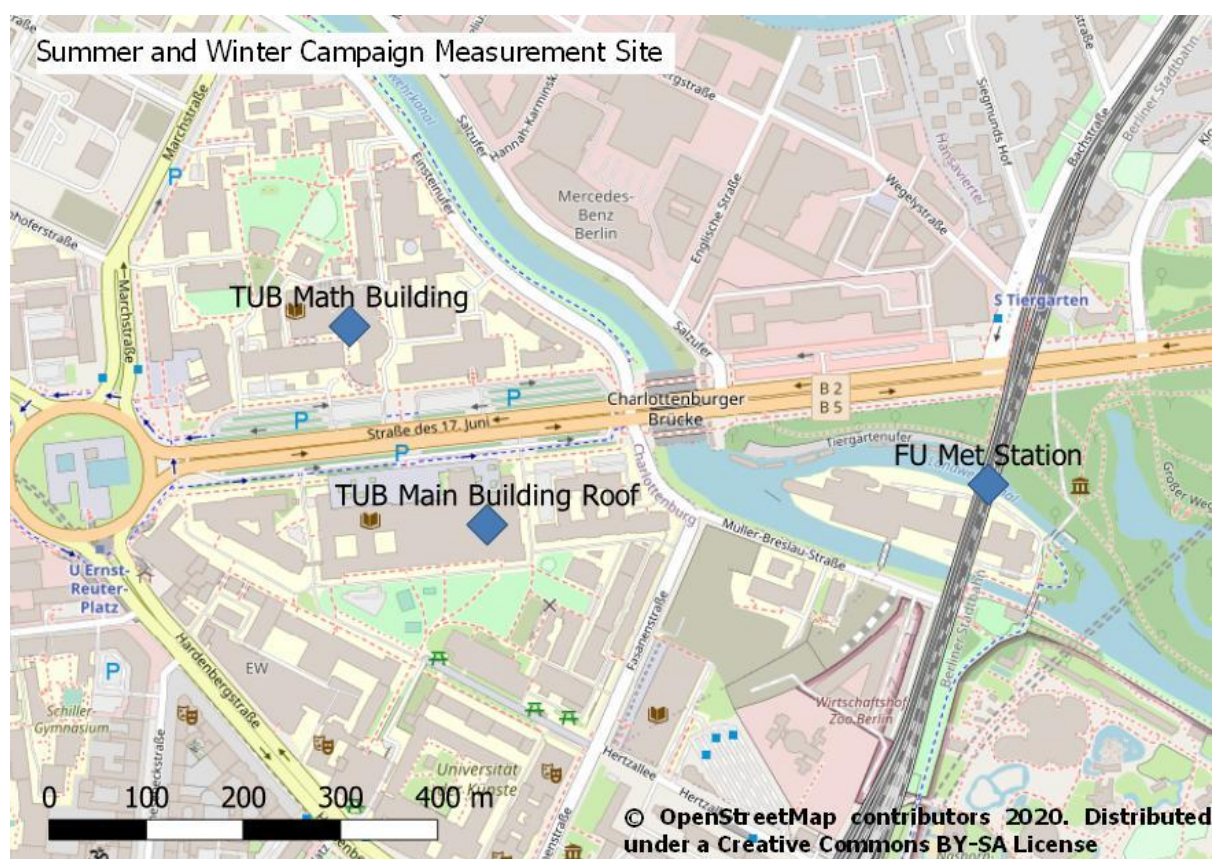
Figure S4. Map of the experimental deployment on and near the campus of the Technical University Berlin (TUB) during the Summer Campaign of 2017 and the Winter Campaign of 2018. The meteorological data provided by the Free University (FU) were collected at the site labeled on the map.

S3. Final results from using s72 in the Winter Campaign, 2018

Table S1. Median R² and RMSE across all test blocks of the best MLR and RF models using internal and ambient T and RH for NO_2. RMSE and MAE are reported in units of ppb.

	NO_2	Median R^2	Median RMSE	Median MAE
MLR	$NO_2 \sim \log(Oxa) * O3a * RH_{amb} * (1/T_{amb})$	0.55	4.13	3.05
	$NO_2 \sim \log(Oxa) * O3a * RH_{int} * (1/T_{int})$	0.55	4.13	3.08
RF	$NO_2 \sim Oxa + O3a + RH_{amb}$	0.53	4.35	3.36
	$NO_2 \sim Oxa + O3a + T_{int}$	0.53	4.17	3.25

Table S2. Median R² and RMSE across all test blocks of the best MLR and RF models using internal and ambient T and RH for O_3. RMSE and MAE are reported in units of ppb.

	O_3	Median R^2	Median RMSE	Median MAE
MLR	$O_3 \sim \log(Oxa) * O3a * (1/RH_{amb}) * T_{amb}$	0.74	4.62	3.75
	$O_3 \sim \log(Oxa) * O3a * (1/RH_{int}) * T_{int}$	0.72	5.16	4.17
RF	$O_3 \sim Oxa + O3a + T_{amb}$	0.79	4.21	3.13
	$O_3 \sim Oxa + O3a + T_{int} + RH_{int} + ToD$	0.94	2.60	2.04

Table S3. Results of RF and MLR models for NO_2 trained with co-location 1, co-location 2, or a combination of both when tested on the Experiment 3 for IOP 3. In the lower half of the table, the models are trained with the same datasets but are tested on Experiment 3 with data points outside the ranges of each training dataset filtered out.

Formula	Co-location 1		Co-location 2		Both co-locations	
NO_2	R^2	RMSE	R^2	RMSE	R^2	RMSE
$NO_2 \sim \log(Oxa) + \log(O3a) + RH_{amb} + 1/T_{amb}$	0.54	5.90	**0.69**	**4.55**	0.67	4.68
$NO_2 \sim \log(Oxa) + \log(O3a) + RH_{int} + 1/T_{int}$	0.52	6.01	0.69	4.61	0.66	4.73
$NO_2 \sim Oxa + O3a + T_{amb}$	0.41	6.28	0.63	5.02	0.55	5.44
$NO_2 \sim Oxa + O3a + T_{int}$	0.46	6.05	0.55	5.51	0.59	5.22
NO_2 – filtered						
$NO_2 \sim \log(Oxa) + \log(O3a) + RH_{amb} + 1/T_{amb}$	0.50	4.80	**0.65**	**4.52**	0.64	4.64
$NO_2 \sim \log(Oxa) + \log(O3a) + RH_{int} + 1/T_{int}$	0.49	4.84	0.65	4.60	0.64	4.69
$NO_2 \sim Oxa + O3a + T_{amb}$	0.42	5.13	0.63	4.77	0.55	5.15
$NO_2 \sim Oxa + O3a + T_{int}$	0.43	5.07	0.54	5.20	0.58	5.04

Table S4. Results of RF and MLR models for NO_2 trained with co-location 1, co-location 2, or a combination of both when tested on Experiment 3 for IOP 3. In the lower half of the table, the models are trained with the same datasets but are tested on Experiment 3 with data points outside the ranges of each training dataset filtered out.

Formula	Co-location 1		Co-location 2		Both co-locations	
O_3	R^2	RMSE	R^2	RMSE	R^2	RMSE
$O_3 \sim Oxa + 1/O3a + RH_{amb} + T_{amb}$	0.76	6.28	0.81	8.53	0.73	4.76
$O_3 \sim Oxa + 1/O3a + RH_{int} + T_{int}$	0.80	5.90	0.82	7.88	0.72	4.79
$O_3 \sim Oxa + O3a + T_{amb}$	0.83	4.67	0.85	7.59	0.85	4.27
$O_3 \sim Oxa + O3a + T_{int}$	0.87	3.91	0.93	4.43	**0.96**	**2.12**
O_3 – filtered						
$O_3 \sim Oxa + 1/O3a + RH_{amb} + T_{amb}$	0.81	3.88	0.81	8.51	0.73	4.69
$O_3 \sim Oxa + 1/O3a + RH_{int} + T_{int}$	0.82	3.92	0.82	7.88	0.73	4.66
$O_3 \sim Oxa + O3a + T_{amb}$	0.90	2.27	0.84	7.57	0.84	4.30
$O_3 \sim Oxa + O3a + T_{int}$	0.92	2.06	0.92	4.46	**0.96**	**2.12**
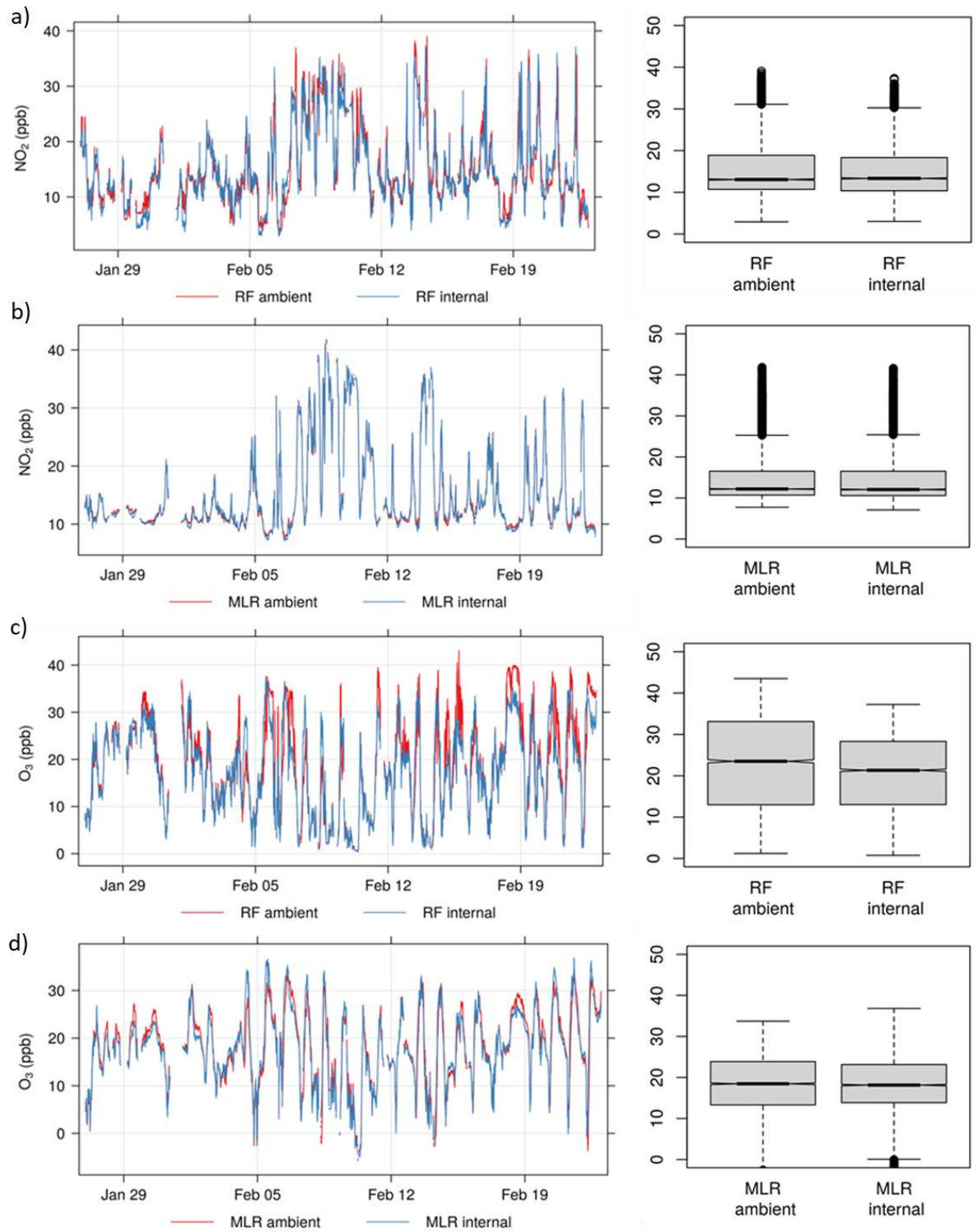
Figure S5. Time plots and histograms for IOP 3 Experiment 3 of a) predicted vs. reference NO_2 concentrations using the RF model, b) predicted vs. reference NO_2 concentrations using the MLR model, c) predicted vs. reference O_3 concentrations using the RF model, d) predicted vs. reference O_3 concentrations using the MLR model. 'Ambient' and 'internal' refer to the use of ambient or internal T and RH data in each model.
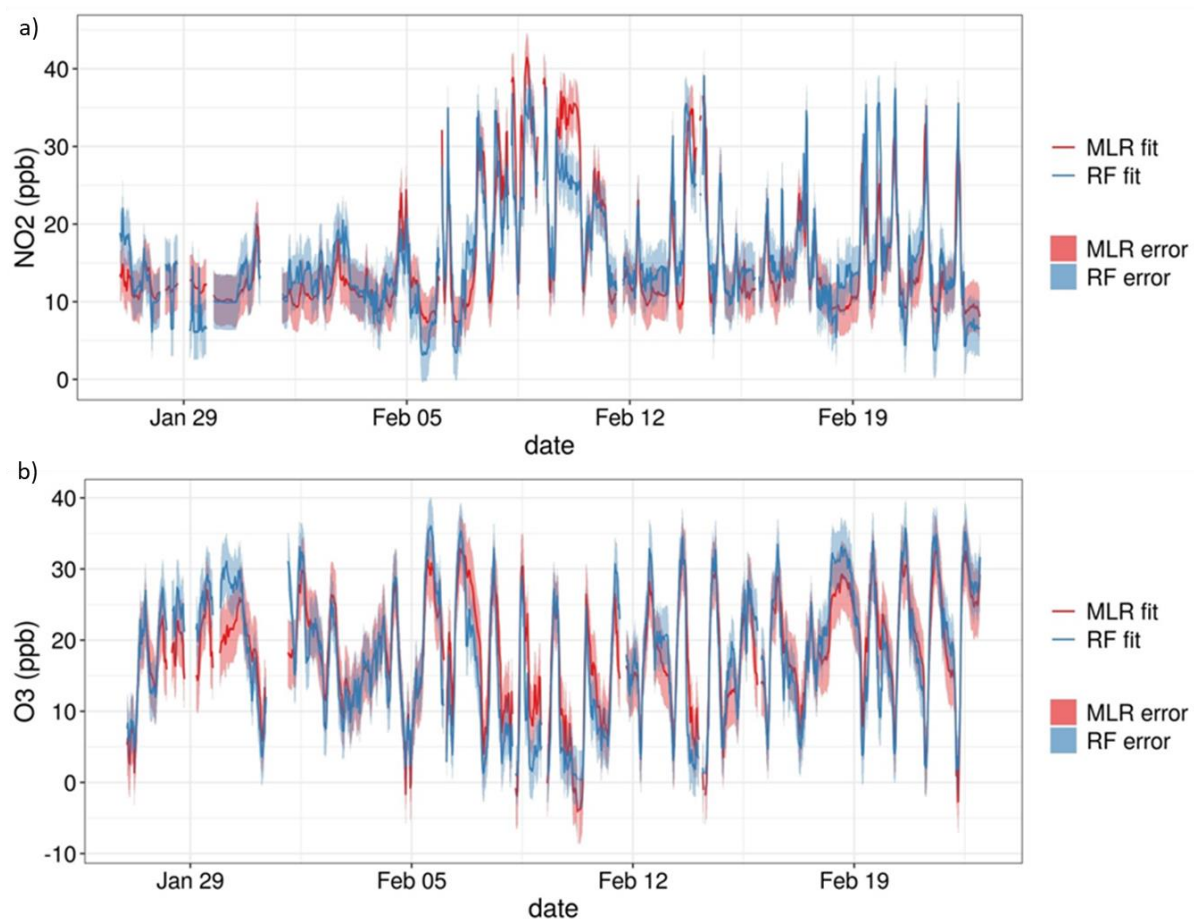
Figure S6. Time plots of both MLR and RF predictions for IOP 3 Experiment 3 including the 95% confidence intervals as shaded regions for a) NO₂ and b) O₃. Data were averaged to 30 minute resolution.
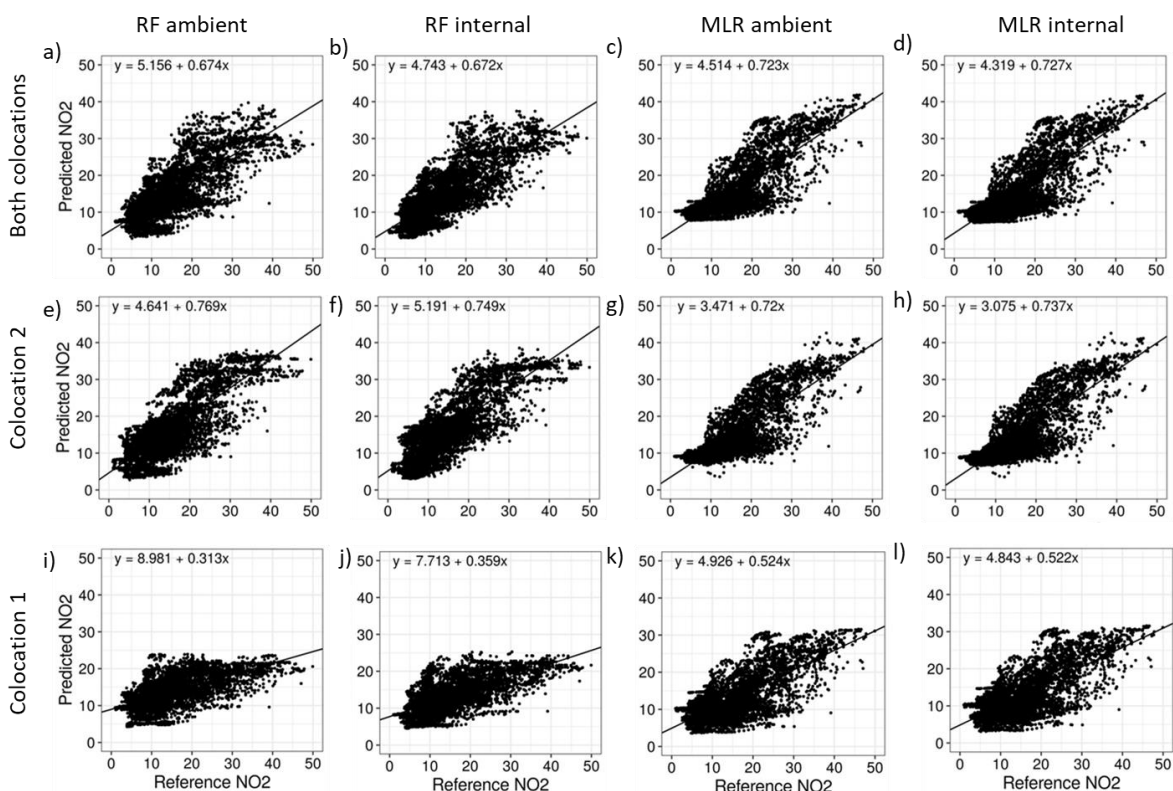
Figure S7: Scatter plots of predicted NO_2 versus reference NO_2 concentrations for Experiment 3 in the Winter Campaign using MLR and RF models trained with co-location 1 (i-l), co-location 2 (e-h), and both combined (a-d). All concentrations are reported in ppb.
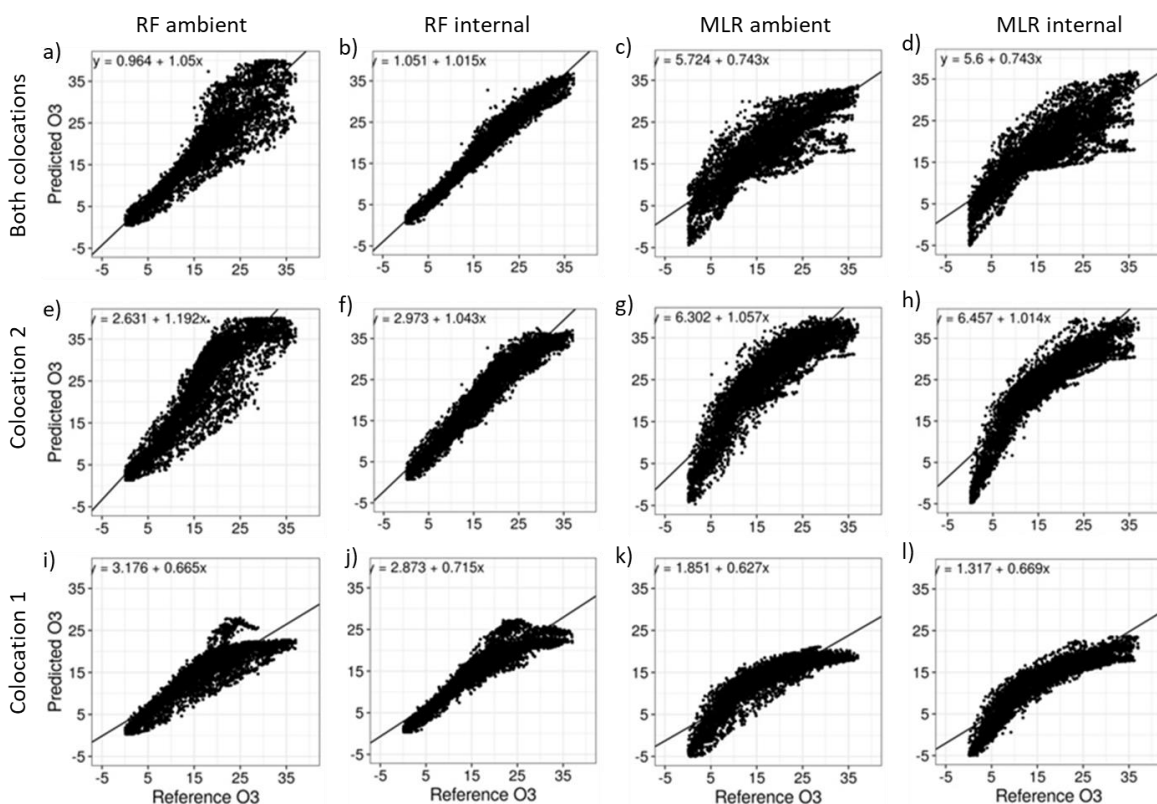
Figure S8: Scatter plots of predicted O_3 versus reference O_3 concentrations for Experiment 3 in the Winter Campaign using MLR and RF models trained with co-location 1 (i-l), co-location 2 (e-h), and both combined (a-d). All concentrations are reported in ppb.